Journal of Wasit for Science and Medicine 2026: 19, (2), 68-75

Pitting Corrosion Resistance of 316L Stainless Steel in Physiological and Marine Chloride Environment

Zeena Razaq Katoof

Department of Chemistry, College of Science, Wasit University, Wasit, Iraq.

Abstract

This experiment compares the pitting corrosion resistance of 316L stainless steel in two chloride environments, 3.5 wt.% NaCl, simulated seawater, and phosphate-buffered saline (PBS), which is a physiological medium, in potentiodynamic polarization and electrochemical impedance spectroscopy (EIS). Findings point to the conclusion that the PBS + NaCl solution is more violent with the passive film of the 316 L stainless steel. An experiment with potentiodynamic polarization indicated that this electrolyte had a lower pitting potential than sal-ammoniac and indicated that the electrolyte was more subject to the initiation of pits. EIS analysis confirms these results with the lowering of the charge transfer resistance and changed capacitive behavior, which was evidence of the formation of a thinner, less stable, and more defective passive film. Quantitative analysis of the electrochemical behavior was done through equivalent circuit models with a constant phase element (CPE). In general, the integrated electrochemical measures indicate that, despite the overall good corrosion performance of 316L stainless steel, the passive film is more prone to localized corrosion in compound chloride-rich environments, including physiological fluids. Such intuitions are essential in the choice of materials and determining the risk of corrosion in the engineering of marine structures and biomedical implants.

Keywords: AISI 316L Stainless Steel, Chloride Corrosion, Potentiodynamic Polarization, and Pitting Corrosion.

1. Introduction

Corrosion damage engineering materials but localized corrosion like pitting can be more harmful. Pitting corrosion is the most localized form of corrosion where the passive film locally disintegrates, resulting in the rapid penetration of the metal and in certain circumstances this also causes an

abrupt fracture in the structural integrity of the material with a minimal amount of material being lost. The much-used type of stainless steel is the austenitic stainless steel, which includes 316L stainless steel because it provides good corrosion resistance since the austenitic forms a protective layer of chromium oxide (Cr_2O_3) passive layer on the surface.

Nevertheless, despite this protective film, these alloys can still be vulnerable to pitting corrosion when exposed to aggressive environments, particularly those containing chloride ions [1, 2]. Pitting corrosion initiates localized defects or inclusions (e.g. MnS) within passive oxide film. Chlorides ions adsorb locally disrupt the oxide layer forming a micro anode. The proceeds via a classical autocatalytic cycle; the metal dissolves within the pit according to the resulting metal ions undergo hydrolysis. Increasing the local environment and accelerating rather dissolution ($M = M^{+3} + 3e$-) within the pit. Metallic ions are hydrolyzed to become more acidic

$$Cr^{+3}{}_{(aq)} + H_2O_{(l)} \rightarrow Cr(OH)^{+2}{}_{(aq)} + H^{+}{}_{(aq)}$$

The movement of chloride ions into the pit keeps the balance of charges, and results in concentrated acidic chloride solutions. The dissolution is increased by the extreme local environment, and the rest of the surface is passive (cathode) [3, 4]. Moreover, electrochemical techniques principle new potentiodynamic polarization scans the potential of the working electrode to produce a current potential curve. Where key parameters include, corrosion potential (Ecorr), open-circuit potential, and breakdown/pitting potential (Ep) as the potential at which pitting starts in a stable. The higher the Epit, the nobler (positive) is, which means the greater is the pitting resistance.

On the other hand, repassivation potential (Erep), represents the potential below which prevailing pits cease growing. Electrochemical Impedance Spectroscopy (EIS), Is a method that uses a small AC potential at a series of frequencies. Impedance of the system is discussed in Nyquist and Bode plots. A healthy passive film has capacitive impedance which is often large. EIS may represent the film as an electrical equivalent circuit (EEC) with circuit elements, solution resistance (Rs), film capacitance (Cf) and charge transfer resistance (Rct) [5, 6].

2. Experimental Work

2.1 Materials and Equipment

Working Electrodes (WE) involved 316L stainless steel coupons (1 cm^2 area of

exposure), embedded in epoxy resin. Electrolytes, 3.5 wt.% NaCl (simulated seawater), 0.9 wt.% NaCl + Phosphate Buffered Saline (PBS). Electrochemical Cell involved three electrodes set up. Counter Electrode (CE), Platinum mesh, Reference Electrode (RE), and Calomel Electrode (Saturated Calomel Electrode (SCE). While preparation of surface include samples were ground to 2000 grit SiC, polished using an alumina suspension (1μm), cleaned with acetone/ethanol and rinsed with deionized water [7, 8].

2.2 Experimental Procedure

Monitors Potential (OCP) Open Circuit Monitors involved samples immersion and adjust monitors to 1 hour to reach a steady state. The Electrochemical Impedance Spectroscopy (EIS) included conduct at OCP, in 10 mV sinusoidal perturbation, at 100 kHz to 10 mHz. The potential is scanned form -0.25 V vs. OCP to +1.2 V vs. SCE (or until a rapid increase in current is observed) at scan rate of 1 mV/s. Cyclic Polarization (Optional) technique was applied to determine the re-passivation potential (Erep), a reverse scan is performed from a specific current density until the re-passivation behavior is captured. Post-Test Examination involved evaluate the pit morphology is evaluated using optical microscopy or Scanning Electron Microscopy (SEM) [9, 10].

3. Results and Discussion

The autocatalytic pitting corrosion mechanism is illustrated in (figure 1). Through three main stages, Initiation begins with the local breakdown of passive film at a locality, for example at an inclusion, exposing bare metal that acts as a micro-anode. Inside the Pit (Microenvironment), rapid metal dissolution occurs ($M \rightarrow Mn^{+} + ne^{-}$), accompanied by the inward migration of chloride ions (Cl^{-}) maintain charge neutrality. The hydrolysis of metal chlorides generates excess H^{+} ions, creating a highly acidic and chloride rich environment.

This acidic condition suppresses re-passivation and accelerates metal dissolution, making the process self-sustaining. Outside the pit (cathodic region), electrons released for the anodic reaction are consumed on the surrounding intact passive surface, where oxygen reduction takes place ($O_2+2H_2O + 4e^{-} \rightarrow 4\ OH^{-}$). This reaction maintains an alkaline and passive condition on the external surface [9, 10].

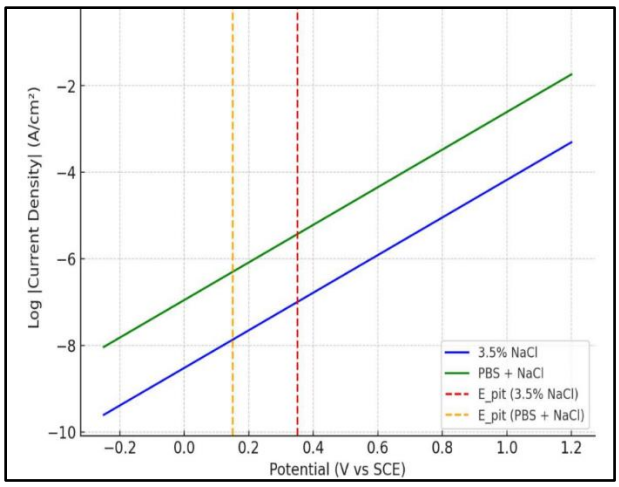

Figure 1: Potentiodynamic polarization curves for 316L in Different Electrolytes.

Electrodynamic polarization curves of 316L stainless steel in various electrolytic solutions illustrated in figure 1. The corrosion behavior in PBS containing NaCl can be explained by several interacting mechanisms. Competitive Adsorption: In PBS+NaCl, chloride (Cl^- out) and phosphate (PO_4^{-3} out) ions are in competition to adsorb on the passive film surface of the metal.

The oxide structure can be locally altered through phosphate adsorption. Weakening the passive film, phosphate ions can form soluble complexes with metal cations (Fe^{+3} and Cr^{+3}) in the passive layer. Leading to reduces the integrity of the oxide film at specific weak points. The local weakening caused by phosphate ions lowers the energy barrier for chloride-induced pitting, resulting in passive film breakdown at a lower applied potential than in pure NaCl solutions [11, 12].

Table 1: Most important electrochemical parameters of the 316L stainless steel in various chloride-containing electrolytes.

Electrolyte	E_corr (V vs SCE)	E_pit (V vs SCE)	Passive Current Density (A/cm²)
3.5% NaCl	-0.25	+0.35	~1 x 10^{-7}
PBS+NaCl	-0.20	+0.15	~5 x 10^{-7}

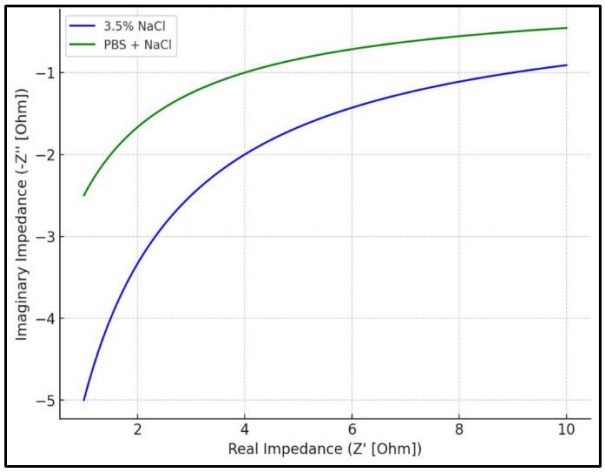

Figure 2: Nyquist plots from EIS data.

The proposed mechanism is corroborated by the smaller semicircle diameter observed in figure 2. Phosphate ions (PO_4^{3-}) in PBS adsorbs onto the passive film, introducing defects and increasing its ionic conductivity. This defective passive layer exhibits lower charge transfer resistance (Rct), facilitating easier penetration by chloride ions and promoting pitting. Consequently, EIS data provides clear

evidence that the passive film is compromised under PBS + NaCl conditions even before the pitting initiation, explaining the observed decrease in the pitting potential (Epit) [13, 14].

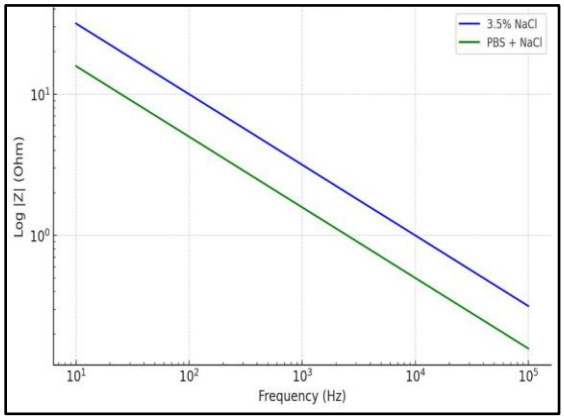

Figure 3: Log |Z| vs. Log f from EIS Data.

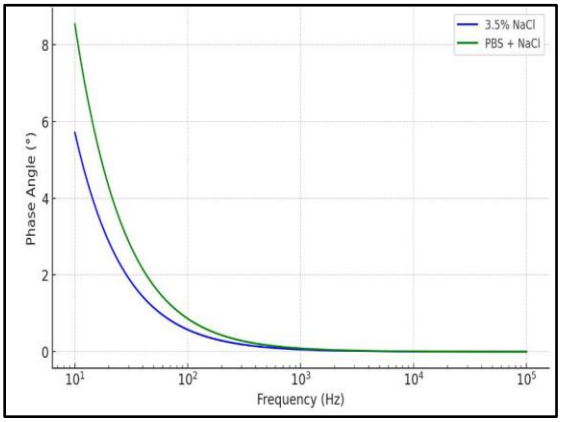

Figure 4: Phase angle vs. Log f from EIS data.

Figures three and four represent bode plots, supplementary evidence of the passive film degradation in PBS+NaCl. Reduced |Z| at low freq, is a direct indication of reduced corrosion resistance (Rct). Wider, lower phase peak, this means that the ideal capacitive behavior is lost because of film modification by phosphate ions. This information perfectly matches the suggested mechanism of phosphate ions adsorb and bind to the oxide film forming a less homogeneous and porous structure. It is a flawed film that is more ionically conductive (lower |Z|) and is not as similar to a perfect capacitor (wider phase peak).

Therefore, offers less protection, allowing it to break down locally earlier on by the chlorides as observed in the lower (Epit) [15, 16]. Moreover, polarization kinetics, included polarization, indicates that the surface corrosion potential (negative) in a sodium chloride-enriched phosphate-salt solution is lower than in ordinary seawater. Indicating reduced corrosion resistance. This is due to the presence of phosphates and other ions in the phosphate-salt solution, which may affect the structure of the passivation layer or chloride absorption. The passivation current density may also increase slightly, suggesting the presence of a permeable layer [17, 18].

Passive film properties of EIS involved the lower charge transfer resistance (Rct) is associated with the smaller diameter of the capacitive arc in the Nyquist plot of PBS+NaCl. This quantitatively validates a weaker passive film, where the non-ideal

heterogeneous structure of the passive film is explained using a Constant Phase Element (CPE) in place of a pure capacitor in the EEC model. CPE exponent n (where n = 1 is a perfect capacitor) can give an insight into the homogeneity of the films [19, 20].

The testing of polarization and Electrochemical Impedance Spectroscopy (EIS) alone offers a complete analysis. EIS defines the integrity of the passive film under normal conditions showing that it is weak in PBS+NaCl. Polarization testing is then used to determine the failure threshold which displays that the weakened film fails under a much lower applied potential [19, 20].

4. Conclusion

This paper has assessed the pitting corrosion resistance of 316L stainless steel in two relevant environments with chloride using electrochemical techniques. Findings reveal that the simulated physiological solution (PBS + NaCl) is more aggressive to the passive film as compared to simple saline which is indicated by lower pitting potential (Epite) and a charge transfer (Rct) resistance value. Under application considerations, Findings underscore the role of choice and design of 316L stainless steel in implementing the stainless steel 316L stainless steel components especially in biomedical implant applications.

5. References

1. Alam M. A., Hossain M. S., and Al-Mamun M., (2024). Influence of chloride concentration and temperature on the pitting corrosion behavior of 316L stainless steel in simulated body fluids. Corrosion Science. 227, 111-123.
2. Chen Y., Wang J., and Li F., (2023). Electrochemical impedance spectroscopy and potentiodynamic polarization analysis of 316L SS in chloride-containing environments: A comparative study. Journal of Electroanalytical Chemistry. 938, 117-129.
3. El-Mahdy G. A., Nishikata A., and Tsuru T., (2021). Electrochemical impedance and potentiodynamic polarization studies of 316L stainless steel in Arabian Gulf seawater. Arabian Journal of Chemistry. 14, 8, 103-115.
4. Fernández-Domene R. M., Sánchez-Tovar R., and García-Antón J., (2023). Localized corrosion of 316L stainless steel in chloride and phosphate environments: A scanning electrochemical microscopy study. Electrochimica Acta. 462, 141-153.

5. Gupta R. K., Singh R., and Birbilis N., (2024). Effect of microstructure on the passive film stability and pitting corrosion resistance of 316L stainless steel in chloride-containing media. Materials and Design. 241, 112-124.
6. Khan M. A., Siddiqi M. N., and Al-Swailem A. M., (2021). Influence of pH and chloride concentration on the electrochemical behavior of 316L stainless steel in simulated cooling water systems. Corrosion Engineering, Science and Technology. 56, 6, 521-532.
7. Kumar P., Singh V., and Tyagi R., (2023). Passive film stability and pitting resistance of 316L stainless steel in phosphate-buffered saline with chloride ions. Materials Chemistry and Physics. 301, 127-136.
8. Li H., Zhang X., and Cao F., (2022). Synergistic effect of chloride and phosphate ions on the degradation of passive films on 316L stainless steel. Electrochimica Acta. 424, 140-152.
9. Liu B., Zhao Y., and Jin Z., (2022). Combined effect of chloride and sulfate ions on the pitting corrosion of 316L stainless steel: An electrochemical noise analysis. Corrosion Science. 209, 110-122.
10. Mouanga M., Bercot P., and De Petris-Wery M., (2022). Application of EIS and localized electrochemical techniques for assessing pitting corrosion in biomedical grade stainless steels. Bioelectrochemistry. 147, 108-119.
11. Oliveira M. C., Feliu S., and Escudero M. L., (2022). Comparative electrochemical study of 316L and 2205 duplex stainless steels in chloride-containing environments using EIS and polarization techniques. Journal of Materials Research and Technology. 18, 2345-2358.
12. Park J., and Lee S., (2022). Effect of surface roughness on the pitting corrosion resistance of 316L stainless steel in marine environments. Corrosion Science. 194, 109-121.
13. Rahman M. M., Peguero J., and Fajardo S., (2021). Electrochemical characterization of 316L stainless steel in simulated seawater and physiological solutions using EIS and cyclic polarization. Journal of Materials Engineering and Performance. 30, 5, 3456-3468.
14. Sánchez-Tovar R., Fernández-Domene R. M., and García-Antón J., (2021). Effect of temperature on the pitting corrosion resistance of 316L stainless steel in chloride solutions: An

electrochemical and microscopic study. Materials Chemistry and Physics. 272, 124-135.

15. Silva R. A., Bastos I. N., and Costa H. R. M., (2021). Constant phase element modeling of passive films on 316L stainless steel in chloride media. Corrosion Science. 178, 108-120.
16. Tian H., Wang C., and Zhang Z., (2022). Passive film properties and pitting resistance of additively manufactured 316L stainless steel in physiological saline. Additive Manufacturing. 55, 102-115.
17. Wang L., Zhang B., and Wu Y., (2020). Mechanistic study of pitting corrosion in 316L stainless steel under combined chloride and phosphate environments. Corrosion Science. 167, 108-119.
18. Zhang X., Liu Y., and Tan Y., (2020). Advanced electrochemical methods for evaluating the pitting resistance of austenitic stainless steels in aggressive media. International Journal of Electrochemical Science. 15, 8, 7892-7905.
19. Zhang C., Yao J., and Zhang, Z. (2026). Machine Learning-Based Pitting Rate Classification and Prediction for 316L Stainless Steel in $NaClO_3$ and NaCl Environment. Materials. 19, 10, 1979.
20. Zhou W., Li J., and He Y., (2023). In-situ electrochemical impedance spectroscopy monitoring of passive film degradation on 316L stainless steel in simulated body fluid. Journal of Electroanalytical Chemistry. 948, 117-129.